

Magnetic and thermal hysteresis in the $O(N)$ -symmetric $(\Phi^2)^3$ model

Madan Rao

Department of Physics, Simon Fraser University, Burnaby, British Columbia, Canada V5A 1S6

Rahul Pandit

Department of Physics, Indian Institute of Science, Bangalore, 560012, India

We extend our study of hysteresis to the $O(N)$ -symmetric $(\Phi^2)^3$ model in three dimensions with the dynamics of the nonconserved order parameter given by a Langevin equation. We analyze both thermal and magnetic hysteresis within this model. We study the systematics of the shapes and areas of hysteresis loops as functions of the amplitude and frequency of the applied field and other parameters in the theory. In the case of magnetic hysteresis we obtain pinched loops for a range of values in parameter space and demonstrate a scaling behavior of the area of the hysteresis loop with the amplitude H_0 of the magnetic field for low amplitudes: $A \approx H_0^\alpha$, where the exponent $\alpha = -\frac{1}{3}$. This puts the magnetic hysteresis behavior of the $(\Phi^2)^3$ model in the same universality class as that of the $(\Phi^2)^2$ model. Thermal hysteresis, obtained by cycling the temperature in the presence of a small magnetic field, is characterized by asymmetric loops. We find that the area of the thermal hysteresis loops scales as a function of the amplitude of the periodic temperature (for low amplitudes): $A \approx T_0^\alpha$, where $\alpha = 1$. We show that our study is relevant to the physics of ferroelectric materials and charge-density-wave systems. Our observations are consistent with existing experimental data on ferroelectrics and charge-density waves.

I. INTRODUCTION

In the past few years^{1,2} there has been a considerable amount of study on nonequilibrium behavior associated with first-order phase transitions. A prototype example of this phenomenon is the growth of domains following a thermal quench of a system from a high-temperature disordered phase to a low-temperature ordered phase. Questions relating to the initial growth of order (nucleation and spinodal decomposition) and the late-stage growth of ordered domains have been focused upon. Relatively little work has been done on the kinetics of driven systems^{3,4} and on systems in the presence of a periodic driving field. In particular, hysteresis, a widely observed phenomenon in experiments, has not received wide attention.

In some recent papers^{5,6} we had initiated a study of hysteresis in simple model-spin systems subjected to periodic magnetic fields. The model-spin systems we investigated were (i) a continuous-spin model in three dimensions where the order parameter is an N -component vector and where the free-energy functional has a $(\Phi^2)^2$ interaction with $O(N)$ symmetry. The dynamics of the nonconserving order parameter is specified by a purely relaxational Langevin equation, (ii) a discrete-spin-lattice model in two dimensions where the order parameter is an Ising spin variable with the Hamiltonian has a nearest-neighbor ferromagnetic coupling. The dynamics of the order parameter is generated by a Monte Carlo single-spin-flip algorithm.

The principal motivation for our study was to construct a nonequilibrium statistical-mechanical theory of

hysteresis in a variety of spin systems where in fluctuations of the order parameter are incorporated. Our theory was used to study the dependence of the shapes and areas of hysteresis loops on the amplitude H_0 and frequency Ω of the magnetic field and on temperature. It made several qualitative predictions which are borne out by experiments on insulating ferrites.⁶ In addition, it made the prediction that the area of the hysteresis loop scales as a power law of the amplitude and frequency of the magnetic field for low values of the amplitude and frequency. We found that the area scales as $H_0^\alpha \Omega^\beta$, where $\alpha = 0.66$ and $\beta = 0.33$ are exponents that are *independent of temperature*. This is in qualitative agreement with the scaling observed in a wide variety of soft magnets. This empirical scaling behavior, known as the Steinmetz law,⁷ suggests that for low values of the magnetic induction B_m (ranging from 500 to 15 000 G in iron) the area goes as⁸

$$A \approx I_m^{B_m^{1.6}}. \quad (1)$$

Our work on the two-dimensional Ising model, though consistent with such scaling behavior, was not extensive enough to extract accurate exponents. Based on these observations we conjectured the existence of universality classes which would be characterized by the same set of exponents α and β . This motivates us to study other spin models and check our "universality hypothesis" (for our reason for expecting scaling, see Sec. I of Ref. 6).

In this paper we extend our analysis of hysteresis to an N -component spin system with $O(N)$ symmetry in three dimensions, whose free-energy functional possesses a $(\Phi^2)^3$ term. As in Ref. 6, the dynamics of the nonconserved order parameter is specified by a purely relaxa-

tional Langevin equation. A distinct feature of the $(\Phi^2)^3$ model is that, in addition to the conventional magnetic-field-driven first-order phase transition, it exhibits a temperature-induced first-order phase transition. We can therefore study the hysteretic behavior of the magnetization either as the field or temperature is cycled periodical-
ly across the phase boundary. On cycling the magnetic field, we obtain pinched hysteresis loops for certain values of the parameters r , u , and v [see Eq. (2) for a definition of these parameters], in addition to loops similar to those obtained in Ref. 6. We see that the constriction in the pinched loops increases as one goes towards the triple line from the ordered phase (see the phase diagram, Fig. 1). This constriction is very prominent when the parameter values are such that the system is initially at equilibrium in the *disordered* phase and when the amplitude of the magnetic field is large. Experiments on the hysteretic response of ferroelectric systems such as Ba-TiO₃ and SbSI (Refs. 9-12) show a similar trend. We find, as in Ref. 6, that the area of the hysteresis loop exhibits a power-law dependence on the amplitude of the magnetic field, for fixed values of the parameters r , u , and v . The scaling, valid for low values of H_0 and f_t , is of the form $A \approx H_0^\alpha$, where $\alpha = 0.60 \pm 0.05$. The exponents α and β seem to be independent of f_t , r , u , and v and equal within error bars to the values obtained in the $(\Phi^2)^2$ model. Thus the magnetic hysteresis behavior of the $(\Phi^2)^3$ theory seems to be in the *same* universality class as that of the $(\Phi^2)^2$ theory. By cycling the temperature across the first-order boundary, we get asymmetric hysteresis loops with very little enclosed area (compared to the loops obtained in magnetic hysteresis). The area of the loops increases with the amplitude of the periodic part of the temperature. We also see that, fixing the amplitude, the area increases as the frequency decreases. This is in qualitative agreement with the behavior of certain charge-density-wave (CDW) systems.¹³ The loops get narrower as one goes towards the tricritical point (see Fig. 1). The area of the thermal hysteresis loops exhibits a power-law scaling with the amplitude of the periodic part of the temperature $A \approx r_0^\alpha$, where $\alpha = 1.0 \pm 0.03$. Thus thermal hysteresis in the $(\Phi^2)^3$ theory seems to be-

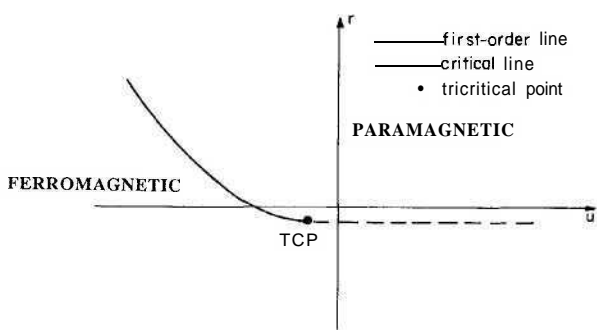


FIG. 1. Schematic phase diagram in the $r-u$ plane for $v < v_c = 16\pi^2$. When an external magnetic field is applied, the first-order boundary develops two first-order wings on either side of the $H=0$ plane.

long to a *different* universality class than magnetic hysteresis in the same model.

In Sec. II we discuss the equilibrium behavior of the $(\Phi^2)^3$ model when $N \rightarrow \infty$. In Sec. III we derive the equations describing the response of the magnetization to a time-varying magnetic field and a time-varying temperature in the large- N limit. Section IV contains the results of our calculations and a discussion of their experimental relevance—both for magnetic and thermal hysteresis. We conclude (Sec. V) with a few additional comments.

II. THE $O(N=\infty)$ -SYMMETRIC, $(\Phi^2)^3$ -THEORY EQUILIBRIUM PROPERTIES

The model we study is an $O(N)$ continuum generalization of the Heisenberg model ($N=3$) in the presence of a magnetic field. The order parameter characterizing the model is an N -component vector $\Phi_\alpha(\mathbf{x}, t)$ (α runs from 1 to N). The model is defined by the free-energy functional

$$\beta F = \int d^3x \left[\frac{1}{2} (\nabla \Phi_\alpha \cdot \nabla \Phi_\alpha) + \frac{r}{2} (\Phi_\alpha \Phi_\alpha) + \frac{u}{4N} (\Phi_\alpha \Phi_\alpha)^2 + \frac{v}{6N^2} (\Phi_\alpha \Phi_\alpha)^3 - \sqrt{N} H_\alpha \Phi_\alpha \right]. \quad (2)$$

We investigate this model explicitly in three spatial dimensions [in Eq. (2) we sum over repeated indices]. The parameters u , v , and H are scaled with appropriate powers of N to obtain a systematic $1/N$ expansion; r is proportional to the deviation of the temperature from the mean-field transition temperature.

We determine the equilibrium phase diagram of the model described by Eq. (2) for $N = \infty$. A lattice version of this model with a different parametrization scheme was analyzed by Emery¹⁴ and Sarbach and Schneider.¹⁵ They obtained the phase diagram in the limit $N = \infty$. The phase diagram of the above model has also been recently analyzed by Lawrie.¹⁶ We present an outline of the calculation in the Appendix—details can be found in Refs. 16 and 17. The model has a low-temperature ferromagnetically ordered phase and a high-temperature paramagnetic phase. The phase diagram depends sensitively on the spatial dimension d —our results are only valid in three dimensions. We concentrate on the section of the phase diagram which exhibits a thermally driven, first-order phase transition ($r, v > 0, u < 0$). We summarize the principal results of the equilibrium properties below.

A. Equilibrium properties when $H = 0$

In $d = 3$, there exists two distinct types of phase diagrams in the $u-r$ plane depending on the value of v . The phases are distinguished by the values of two order parameters, namely $z = N^{-1}(\Phi^2)$ and $M = \langle \Phi \rangle$. For $0 < v < v_c = 16\pi^2$, two phases—the ferromagnetic and the paramagnetic phases—are obtained, as shown schematically in Fig. 1. The two phases will be described below in greater detail. From Fig. 1 we see that the two phases are separated by a first-order phase boundary (represented by a solid line) and a critical line (represented by a

dashed line) which meet at a tricritical point (TCP) at (r_T, u_T) . Thus at fixed v ($< v_c = 16\pi^2$) and u ($< u_T$), an increase in r drives the system from an ordered phase to a disordered phase across a first-order phase boundary. The numerical values of the first-order phase boundary in the r - u plane are given in Table I for $v = 105.2758 > v_c$.

For $v > v_c$, the tricritical point disappears—the two phases are now separated by a first-order line and critical line which meet a critical end point. The first-order line extends farther, ending in an ordinary critical point. We do not exhibit this part of the phase diagram and henceforth v shall always be taken to be less than v_c .

The expressions for the magnetization and the correlation functions to $O(1)$ in a $1/N$ expansion in both the paramagnetic and the ferromagnetic phases are given below. These expressions will be used later as initial conditions for the dynamical equations we derive in Sec. III.

1. Paramagnetic phase

In the high-temperature paramagnetic phase the magnetization (at $H=0$) is zero. By isotropy (in the absence of a magnetic field) all off-diagonal components of the two-point correlation function $C_{\alpha\beta} = \langle \Phi_\alpha(\mathbf{q})\Phi_\beta(-\mathbf{q}) \rangle$ are zero. The diagonal components of the correlation function, namely $C_{\alpha\alpha}(\mathbf{q}) \equiv \langle \Phi_\alpha(\mathbf{q})\Phi_\alpha(-\mathbf{q}) \rangle$, are all equal and nonzero. Averages are taken over the equilibrium thermal distribution. Higher-order cumulants of Φ_α are smaller than $C_{\alpha\alpha}$ by factors of $1/N$. Therefore, in the $N \rightarrow \infty$ limit, these higher-order correlation functions vanish. The diagonal components of the correlation function are given by

$$C_{\alpha\alpha} = 1/(r + q^2 + uS + vS^2) \quad \text{for } \alpha = 1, \dots, N, \quad (3)$$

$$S = \frac{1}{2\pi^2} \int_0^\infty C_{\alpha\alpha} q^2 dq. \quad (4)$$

Since the theory is regularized on a lattice, we take the upper momentum cutoff to be 1. Equations (3) and (4) are solved self-consistently to obtain $C_{\alpha\alpha}$.

TABLE I. Phase boundary in the r - u plane. $v = 105.2758 > 16\pi^2$, $H=0$.

$r=r_f$	$U=u_f$
0.28241	-10.9078
0.38241	-12.7664
0.48241	-14.4883
0.58241	-16.1227
0.68241	-17.7080
0.78241	-19.2594
0.88241	-20.7267
0.98241	-22.0670
1.08241	-23.3083
1.18241	-24.4791
1.28241	-25.5945
1.38241	-26.6639
1.48241	-27.6929

2. Ferromagnetic phase

The low-temperature phase of the theory is an ordered phase in which a spontaneous magnetization M and z develop nonzero expectation values. The thermodynamic quantities and correlation functions in this phase are calculated (see the Appendix) in the presence of an infinitesimal magnetic field in the $\alpha=1$ direction, i.e., $H_\alpha \rightarrow 0^+ \delta_{\alpha 1}$. The spontaneous magnetization M is given by

$$M_\pm = \langle \Phi_1(q) \rangle = (\{-u \pm (u^2 - 4rv)^{1/2}\}/2v) \cdot (1/2\pi^2)^{1/2}, \quad (5a)$$

while

$$z = \langle \Phi^2 \rangle = [-u \pm (u^2 - 4rv)^{1/2}]/2v. \quad (5b)$$

We choose that value of the root for which the free-energy density, given by

$$W(r, u, v, \dots) = \left[-\frac{1}{2}rz + \frac{1}{4}uz^2 - \frac{1}{6}vz^3 - \frac{1}{4\pi^2} \left(\frac{r^2}{9} - \frac{\ln 2}{3} \right) \right],$$

is a minimum. The off-diagonal components of $C_{\alpha\beta}$ are zero (axial symmetry about the ordering direction). The broken-symmetry axis defines a direction in spin space allowing for fluctuations of the order parameter normal to this direction to be different from those parallel to it. The transverse correlation function C_\perp (which is the component perpendicular to the direction of spontaneous magnetization, $\alpha \neq 1$), clearly describes a zero mode, since it is associated with spin-wave fluctuations and hence diverges in the long-wavelength limit,

$$C_{\alpha\alpha}(q) = q^{-2}. \quad (5c)$$

All higher-order cumulants go to zero in the large- N limit.

B. Equilibrium properties when $H \neq 0$

We now turn on a uniform magnetic field along the $\alpha=1$ direction. We will merely investigate the effect of the magnetic field on the phase diagram in Fig. 1. The first-order line develops two symmetrical first-order "wings" on either side of the r - u plane (the H axis points out of the plane of Fig. 1). The first-order freezing temperature $r_f(H)$ therefore depends on the value of the magnetic field. We find (and this is to be expected) that the ordering temperature $r_f(H_1) > r_f(H_2)$ when $H_1 > H_2$. We also find that for a certain range of values of the parameters r and u , a change in the magnetic field drives the system from a paramagnetic phase to a ferromagnetic phase across the first-order wing. The magnetization in the ferromagnetic phase is obtained by solving the following set of self-consistent equations:

$$M = \frac{H}{2\mu^2}, \quad (6a)$$

$$\mu^2 = \frac{1}{2}(r + uz + vz^2), \quad (6b)$$

$$z = \int_0^1 \frac{1}{2\pi^2} \left[\frac{q^2}{(\frac{1}{2}q^2 + \mu^2)} \right] dq + \frac{H^2}{4\mu^4}. \quad (6c)$$

These equations may not lead to a unique solution for M for a fixed choice of parameters. The equilibrium magnetization is the value of M which minimizes the free energy [Eq. (A7)].

From our analysis of the equilibrium phase diagram of the $(\Phi^2)^3$ model we see that there are two distinct first-order phase boundaries: (i) the phase boundary between ferromagnetic and paramagnetic phases traversed by increasing the temperature r [keeping u , v , and H (small) fixed]; and (ii) the phase boundary between the ferromagnetic phase with positive magnetization and the ferromagnetic phase with negative magnetization traversed by changing the magnetic field from positive to negative values through zero (keeping r , v , and u fixed). We study the kinetics of the $(\Phi^2)^3$ model associated with both the first-order phase boundaries by cycling either the temperature or the magnetic field periodically across them. This will lead us to an analysis of thermal and magnetic hysteresis.

III. DYNAMICS OF THE $(\Phi^2\Phi)^3$ THEORY

As we argued in Ref. 6, the order parameter Φ_α is not conserved and its evolution in time is governed by a Langevin equation. Thermal fluctuations are mimicked by a random noise (whose time scale of variation is much smaller than the time scale of relaxation of the magnetization). The Langevin equation is

$$\frac{d}{dt}\Phi_\alpha(\mathbf{x},t) = -\frac{\delta(\beta F)}{\delta\Phi_\alpha(\mathbf{x},t)} + \eta_\alpha(\mathbf{x},t), \quad (7)$$

where βF is given by Eq. (2). The noise η is a Gaussian white noise with the following statistics:

$$\begin{aligned} \langle \eta_\alpha(\mathbf{x},t) \rangle &= 0, \\ \langle \eta_\alpha(\mathbf{x},t)\eta_\beta(\mathbf{x}',t') \rangle &= 2\Gamma\delta(\mathbf{x}-\mathbf{x}')\delta(t-t')\delta_{\alpha\beta}. \end{aligned}$$

Γ is a microscopic kinetic coefficient, which we take to be independent of q since Φ is nonconserved. Γ can be estimated from linewidth measurements in ferromagnetic (electric) resonance.

Starting from Eq. (7), we can derive an infinite hierar-

chy of dynamical equations in the n -point correlation functions of $\Phi_\alpha(\mathbf{x},t)$. In the limit $N \rightarrow \infty$ this infinite set of different equations is truncated.

In order to derive the dynamical equations for the moments of $\Phi(\mathbf{x},t)$, we substitute the model free-energy functional Eq. (2) into the Langevin equation Eq. (7). In momentum space we get

$$\begin{aligned} \frac{d}{dt}\Phi_\alpha(\mathbf{q},t) &= -(r+u^2)\Phi_\alpha(\mathbf{q},t) + (u/N)V_3 \\ &\quad + (v/N^2)V_5 + H\delta_{\alpha,1}\delta_{q,0}] + \eta_\alpha(\mathbf{q},t), \end{aligned} \quad (8)$$

where

$$\begin{aligned} V_3 &= \int \int \Phi_\alpha(\mathbf{q}-\mathbf{q}_1,t)\Phi_\beta(\mathbf{q}_1-\mathbf{q}_2,t)\Phi_\beta(\mathbf{q}_2,t)d^3q_1d^3q_2, \\ V_5 &= \int \int \int \Phi_\alpha(\mathbf{q}-\mathbf{q}_1,t)\Phi_\beta(\mathbf{q}_1-\mathbf{q}_2,t)\Phi_\beta(\mathbf{q}_2-\mathbf{q}_3,t) \\ &\quad \times \Phi_\gamma(\mathbf{q}_3-\mathbf{q}_4,t)\Phi_\gamma(\mathbf{q}_4,t) \\ &\quad \times d^3q_1d^3q_2d^3q_3d^3q_4, \end{aligned}$$

and repeated indices imply a summation from 1 to N .

Magnetic hysteresis is obtained when the magnetic field is cycled periodically in the $a=1$ direction of spin space, i.e., $H_a = H_0 \sin(\Omega t) \delta_{\alpha,1}$. *Thermal hysteresis* is obtained when the temperature $r(t) = r_f + \frac{1}{2}r_0 \cos(\Omega t)$ (here r_f is the ordering (first-order transition) temperature, and r_0 is the amplitude of the oscillating part of the temperature). We derive kinetic equations for both these cases in the $N \rightarrow \infty$ limit. The details of the derivation can be obtained from Refs. 6 and 17.

A. Magnetic hysteresis

When the magnetic field is varied periodically, the magnetization responds periodically but with a phase lag and higher harmonics. The dynamics of the magnetization $M = \langle \Phi_1(\mathbf{q},t) \rangle$ can be obtained by taking averages with respect to the noise $\eta_\alpha(\mathbf{q},t)$ of all the terms in Eq. (8). Thus

$$\begin{aligned} \frac{d}{dt}M(\mathbf{q},t) &= -\Gamma \left[(r+q^2)M(\mathbf{q},t) + \frac{u}{N} \int \int \langle \Phi_\alpha \Phi_\beta \Phi_\beta \rangle d\mathbf{q}_1 d\mathbf{q}_2 \right. \\ &\quad \left. + \frac{v}{N^2} \int \int \int \langle \Phi_\alpha \Phi_\beta \Phi_\beta \Phi_\gamma \Phi_\gamma \rangle d\mathbf{q}_1 d\mathbf{q}_2 d\mathbf{q}_3 d\mathbf{q}_4 + H\delta_{\alpha,1}\delta_{q,0} \right]. \end{aligned} \quad (9)$$

In Ref. 6 we had shown that if the dynamics of the order parameter is governed by Eqs. (2) and (7), then the magnetization of the n -point correlation functions will be translational invariant at all times provided the magnetization and the n -point correlation functions at $t=0$ are translationally invariant. Thus in the present study the magnetization will be homogeneous at all times and therefore the q dependence of $M(t)$ can be dropped. Our initial conditions are such that the magnetization points

along the $a=1$ direction of spin space. The above dynamical equations, with the field in the $a=1$ direction, maintain this orientation of the magnetization (see Ref. 6 for a derivation). Thus the $\alpha \neq 1$ components of $\langle \Phi_\alpha(\mathbf{q},t) \rangle$ are equal to zero at all times. For $N \rightarrow \infty$ the three-point and five-point correlation functions factor exactly into products of one-point and two-point correlation functions.

Also,

$$\sum_{\alpha=1}^N \langle \Phi_\alpha \Phi_\alpha \rangle = \sum_{\alpha \neq 1}^N \langle \Phi_\alpha \Phi_\alpha \rangle + \langle \Phi_1 \Phi_1 \rangle \\ = (N-1)C_\perp + C_\parallel , \quad (10)$$

whence we see that $I(1/N)\sum_\alpha \langle \Phi_\alpha \Phi_\alpha \rangle$ is simply C_\perp in the limit $N \rightarrow \infty$. Thus, for $N = \infty$,

$$\frac{dM}{dt} = \frac{1}{2} [A(t)M(t) + H(t)] , \quad (11a)$$

$$A(t) = -(r + uM^2 + uS + vM^4 + 2vM^2S + vS^2) , \quad (11b)$$

$$S(t) = \frac{1}{2\pi^2} \int_0^1 q^2 C_\perp(q, t) dq , \quad (11c)$$

$$\frac{d}{dt} C_\perp(q, t) = -[q^2 - A(t)]C_\perp(q, t) + 1 , \quad (11d)$$

$$H(t) = H_0 \sin(\Omega t) , \quad (11e)$$

where the $\langle \eta_\alpha(\mathbf{q}, t) \Phi_\alpha(-\mathbf{q}, t) \rangle$ term is evaluated using Noviko's theorem,¹⁸ which is valid for a Gaussian white noise. In the above equations we measure time in units of $(2\Gamma)^{-1}$. Equations (11a–11e) are the set of two closed integro-differential equations that describe exactly the time evolution of our model Eq. (7) for $N = \infty$. It can be easily verified that the stationary solutions of these equations are precisely the equilibrium values of the magnetization and the transverse correlation function, Eq. (5).

The initial conditions required for the solution of these differential equations are the equilibrium values of M and C_\perp . This set of equations has to be solved numerically. We have used an Euler method and a Runge-Kutta method to solve the differential equations and a 20-point Gaussian quadrature for the integral. We obtain analytical solutions in the large- Ω limit. We present the results for magnetic hysteresis in Sec. IV A.

B. Thermal hysteresis

To study thermal hysteresis we work with a very small, constant magnetic field H in the $a=1$ direction. Thus the $\alpha=1$ component of $\langle \Phi_\alpha(\mathbf{q}, t) \rangle$ is nonzero at $t=0$. The $\alpha \neq 1$ components are zero at $t=0$ [Eqs. (6)] and consequently remain zero at all times. At $t=0$, we begin with the system in equilibrium in the paramagnetic phase with a magnetic field H and $r(H) > r_f(H)$, where r_f , the first-order transition temperature, depends on H , u , and v (Fig. 1). We now subject the spin system to a periodically varying temperature that takes it back and forth across the first-order wing of Fig. 1 (keeping u , v , and H fixed).

The equations describing the time evolution of the magnetization are

$$\frac{d}{dt} M(t) = \frac{1}{2} [A(t)M(t) + H] , \quad (12a)$$

$$A(t) = -[r(t) + uM^2 + uS + vM^4 + 2vSM^2 + vV^2] , \quad (12b)$$

$$S(t) = \frac{1}{2\pi^2} \int_0^1 q^2 C_\perp(q, t) dq , \quad (12c)$$

$$\frac{d}{dt} C_\perp(q, t) = -[q^2 - A(t)]C_\perp(q, t) + 1 , \quad (12d)$$

$$r(t) = r_f + \frac{1}{2} r_0 \cos(\Omega t) , \quad (12e)$$

and $r(0) = r_f + \frac{1}{2} r_0$ such that the system is in the paramagnetic phase at $t=0$. The initial conditions for M and C_\perp are given by Eqs. (6). For general values of the parameters, Eqs. (12a)–(12e) have to be solved numerically [the numerical codes are the same as the ones used to solve Eqs. (11)]. Once again, analytical solutions can be obtained in the large- Ω limit. Our results for thermal hysteresis are given in Sec. IV B.

IV. NUMERICAL RESULTS

A. Magnetic hysteresis

1. Evolution of shapes and hysteresis loops as a function of H_0 and Ω

The dynamical equations Eqs. (11) can be solved to obtain the shape of the hysteresis loop as a function of the amplitude and frequency of the magnetic field at all points in the phase diagram (Fig. 1). We choose the temperature r and coupling u (in our computation we keep v fixed and equal to 105.2758) such that the spin system is initially (time $t=0$) at equilibrium in the ferromagnetic phase (with $H_\alpha = \epsilon \delta_{\alpha,1}$ and $\epsilon \rightarrow 0^+$). As the field is cycled, we go past the first-order phase boundary (surface) at $H=0$. We fix H_0 , the amplitude of the magnetic field, and monitor the shape of the hysteresis loop as a function of Ω , the frequency of the magnetic field. For a generic point (r, u) in the phase diagram [corresponding to the ferromagnetic phase, and away from the first-order boundary (dotted line in Fig. 1) in the $r-u$ plane], the shapes follow the same sequence of changes as observed in the $O(N=\infty)$, $(\Phi^2)^2$ theory (Ref. 2): from a low-frequency, spindle-shaped hysteresis loop to a high-frequency elliptical loop in the upper half of the $M-H$ plane. Since these results are the same as those we obtained for the $(\Phi^2)^2$ theory,^{1,2} we refer the reader to Ref. 2 for a detailed account of them. However, we reiterate some of the conclusions of Ref. 2: mean-field hysteresis [obtained by dropping C_\perp from Eq. (11)] can occur only if $H > H_{sp}$ (the mean-field spinodal field, which is many orders of magnitude greater than experimentally accessible fields); to obtain symmetric hysteresis loops (i.e., the loop must be symmetric when $H \rightarrow -H$ and $M \rightarrow -M$) for low-field amplitudes, one needs to include fluctuations of the order parameter (via C_\perp in the $N=\infty$ limit we consider).

2. Shape as a function of parameters r and u : pinched hysteresis loops

We now investigate the changes in the shape of the hysteresis loop when r and u are varied across the phase diagram (Fig. 1; u is held fixed and less than V_c for convenience). We do not consider values of v larger than v_c , since the only qualitative change in the phase boundary occurs in the neighborhood of the tricritical point while leaving the triple line largely unaltered. A typical hysteresis loop (denoted as type-1 hysteresis loop in the

classification scheme of Ref. 6) is shown in Fig. 2. The values of the parameters r and u for which such a spindle-shaped loop is obtained are such that the system is away from the triple line (in the ferromagnetic phase). For values of r and u close to the first-order phase boundary, we notice these hysteresis loops develop a slight constriction near $M=0$. This can be understood by the following the mechanical analogy [discussed in Ref. 6 for a $(\Phi^2)^2$ model]. Consider a particle moving in a potential of the form

$$V(x)=ax^2+bx^4+cx^6,$$

where $a, c > 0$ and $b < 0$. This potential has three minima at $x=x_0^+$, 0, and x_0^- where $XQ = -x_0$. At $t=0$, let the particle be at $x=x_0^+$. This corresponds to a positive magnetization $M=M_{eq}$ in our model. We now apply a homogeneous, periodic field which couples linearly to x :

$$V(x,t)=ax^2+bx^4+cx^6-xH_0\sin(\Omega t).$$

As time evolves, the field goes from positive H_0 to negative H_0 and the particle decays¹⁹ from x_0^+ to the x_0^- minimum. For high H_0 , low f_t and large r [close to the coexistence curve in the $(\Phi^2\Phi)^3$ theory], the particle goes from x_0^+ to the $x=0$ minimum before decaying into the x_0^- minimum. The time spent in the $x=0$ minimum depends on r . The large time spent near $x=0$ (when r is large) is reflected in the constriction of the $M-H$ curve. These loops are termed pinched hysteresis loops and are observed in several ferroelectrics such as BaTiO₃.

As we approach the tricritical point, the loops become narrower and their areas decrease. This is because the equilibrium magnetization decreases (this reduces the remnant magnetization) and fluctuations become more pronounced (this reduces the coercive field) as we approach the tricritical point.

Let us now choose the parameters r and u such that

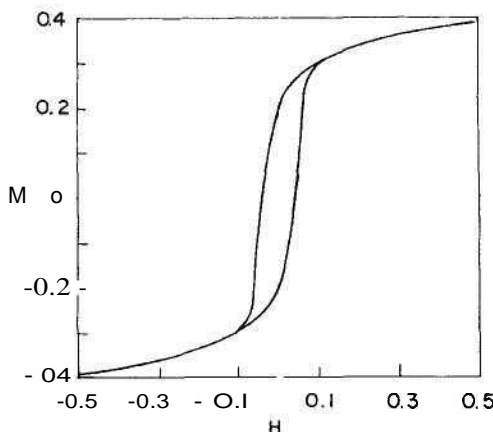


FIG. 2. A typical magnetic hysteresis loop. At $t=0$, the system is in the ferromagnetic phase. The parameters are $r=0.3$, $u=-10.9078$, and $u=105.2758$. The amplitude $H_0=0.5$ and frequency $\Omega=5 \times 10^{-3}$.

the spin system is initially $t=0$ and therefore $H(t)=0$ in the high-temperature paramagnetic phase. The first-order boundary (encountered while changing H , but keeping r and u fixed) is situated at a *nonzero* value of the field, $H_F(r,u)$ (this corresponds to the first-order wings coming out of the plane of Fig. 1; see Sec. II B). Therefore if the amplitude H_0 is made larger than $H_F(r,u)$, the spin system goes from a paramagnetic phase to a ferro "up" phase, back to the paramagnetic phase, and then to the ferro "down" phase. The constriction in the hysteresis loops generated by such a cycle is very pronounced. Figure 3 shows how loops of type 1 (in the classification scheme discussed in Ref. 6) change their shapes as a function of increasing r (u is held fixed). We see that for low r and high H_0 , the pronounced constriction leads to the appearance of double hysteresis loops. This behavior is exhibited by various ferroelectric materials and should be compared with the experimental loops of Merz⁹ for BaTiO₃ and Kawada¹² for SbSI (see Figs. 5 and 6). In particular note that our theory successfully describes the trend of the variation of the shapes as a function of temperature.

3. Scaling of the area of the hysteresis loop

Given a hysteresis loop, we can easily determine its area. The area of the loop is a measure of the work done in cycling the magnetic field through one cycle. Let us fix the parameters r , u , and v and the frequency f_t . The area of the loops should increase as a function of H_0 . Since our model does not have fixed-length spins, the magnetization does not saturate completely, though the area is bounded. We shall restrict ourselves to small H_0 , i.e., $H_0 \ll H_{sp}$, where H_{sp} is the mean-field spinodal field. We find that the area of the asymptotic hysteresis loops scales with H_0 as

$$A \propto H_0^\alpha,$$

where $\alpha=0.60 \pm 0.05$. Figure 4 exhibits this scaling for a wide range of amplitudes and frequencies of the field. This exponent is, as far as we can tell, independent of the frequency f_t (for low frequency) and the parameters r , u , and v (as long as we are in the same region of the phase diagram). We thus conclude that for low values of H_0 and f_t , the area $A \approx \xi(r,u,v,\Omega)H_0^\alpha$. This exponent should be compared with the scaling exponents obtained in the $(\Phi^2)^2$ model. There we find (Ref. 6) that the area of the hysteresis loop scales as a function of both the amplitude and the frequency of the field as

$$A \approx H_0^\alpha \Omega^\beta,$$

where α and β are consistent with $\frac{2}{3}$ and $\frac{1}{3}$, respectively. In our study of the $(\Phi^2)^3$ theory, we have not investigated the scaling behavior with respect to the frequency. We thus see that without our error bars, the magnetic hysteresis behavior of the $(\Phi^2)^3$ model seems to be in the same "universality class" as the hysteresis (magnetic) behavior of the $(\Phi^2)^2$ model.

4. Analytical results in the high-frequency limit

Equations (11) can be solved analytically in the high-frequency limit by taking a Fourier transform with respect to t . This converts the set of nonlinear differential equations into a set of nonlinear integral equa-

tions. These integral equations can be solved iteratively for the Fourier-transformed magnetization $\tilde{M}(\omega)$ and transverse correlation function $C_{\perp}(q, \omega)$. This is equivalent to a large- Ω expansion. The first iterates of $\tilde{M}(\omega)$ and $\tilde{C}_{\perp}(q, \omega)$ are given by

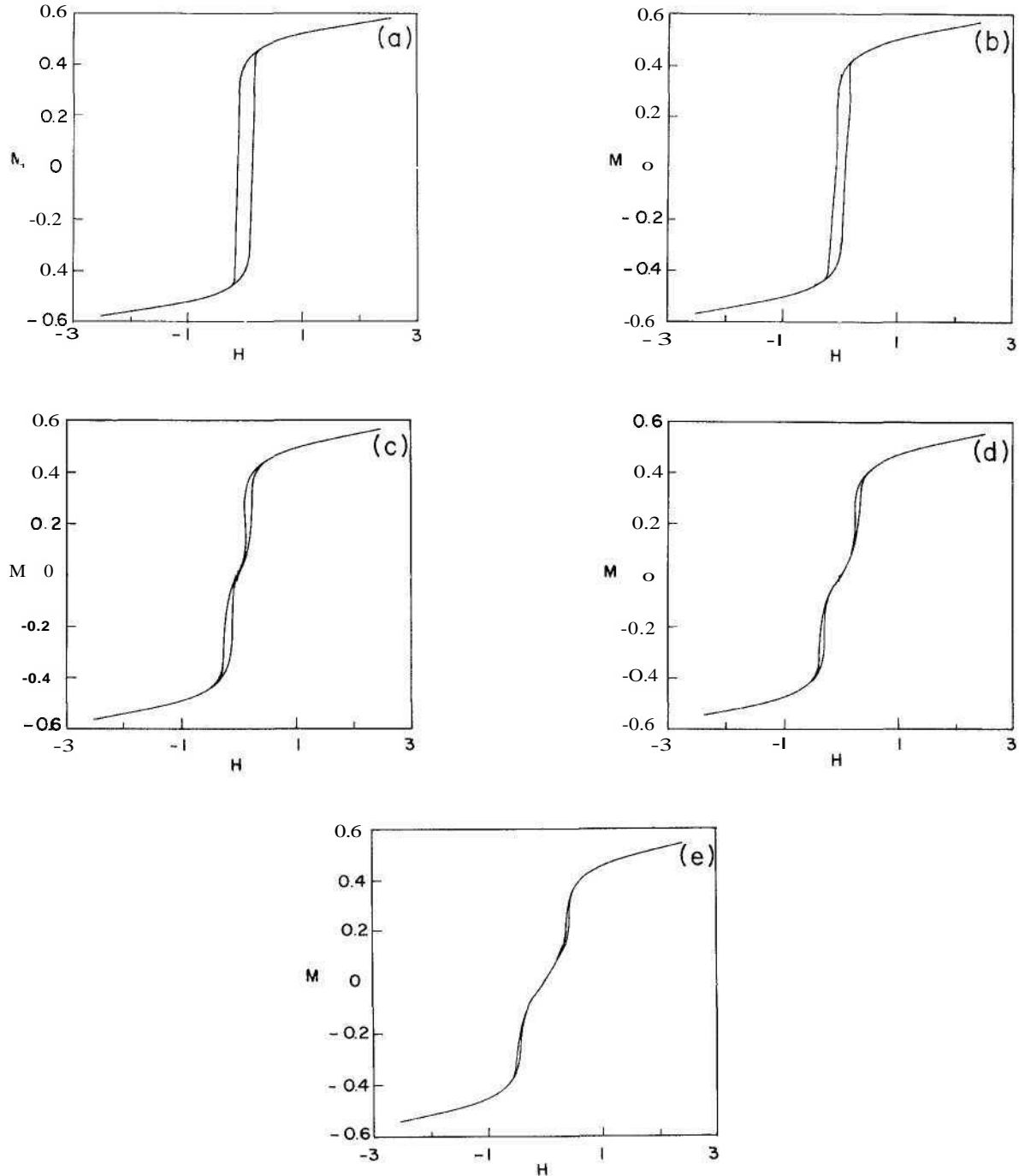


FIG. 3. Evolution of pinched and double hysteresis loops with increasing r . H_0 and f_t are held fixed ($H_0 = 2.5$ and $f_t = 2 \times 10^{-3}$). The parameters u ($= -25.59$) and v ($= 105.2758$) are also kept constant. The pinched constriction becomes more pronounced as one nears the coexistence curve (from the ferromagnetic side) and crosses into the paramagnetic phase: (a) $r = 1$, (b) $r = 1.5$, (c) $r = 2$, (d) $r = 2.5$, and (e) $r = 3$.

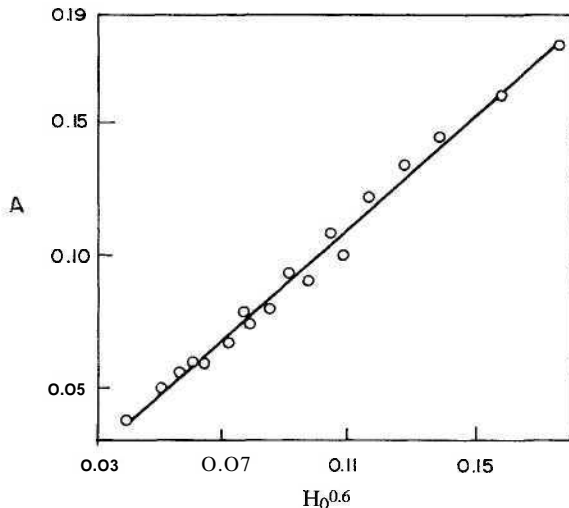


FIG. 4. Area of the hysteresis loop as a function of the amplitude H_0 . The exponent $\alpha=0.6$ is found to be independent of f_t , r , u , and v . The scaling is valid for low H_0 ($< H_{sp}$) and f_t .

$$\tilde{M}_1(\omega) = (H_0/4\Omega)[\delta(\omega + \Omega) - \delta(\omega - \Omega)] \quad (13a)$$

and

$$\tilde{C}_1^1(q, \omega) = 0. \quad (13b)$$

We see that, in the large- Ω limit, $M(t)$ has the same frequency as $H(t)$, but is phase shifted. This gives an elliptical hysteresis loop in the upper half [since $M(t=0>0)$] of the M - H plane. The area of the hysteresis loops is given by

$$A = \int_0^{2\pi/\Omega} M(t) \frac{dH}{dt} dt = -\pi H_0^2 / 8\Omega. \quad (14)$$

We thus see that for large Ω the shapes of the hysteresis loops are elliptical and do not possess a constriction at $M=0$. Moreover, it is obvious from considering higher iterates of the solution of the integral equation that only odd harmonics contribute to the magnetization profile at lower frequencies. We also see that for high frequencies the area of the loop scales as $H_0^2 \Omega^1$, which is the same high-frequency scaling seen in the $(\Phi^2)^2$ model. This further leads credence to our assertion that the two models belongs to the same universality class regarding magnetic hysteresis.

5. Experimental status

The three-component $(\Phi^2)^3$ model provides a useful description for phase transitions in displacive ferroelectrics. The order parameter describing the ferroelectric phase transition is the electric polarization vector P . The equilibrium behavior of these ferroelectrics (strictly speaking, if the unpolarized crystal has a center of inversion symmetry) is described by the well-known Devonshire theory:²⁰

$$F = r(P \cdot P) + B(P \cdot P)^2 + C(P \cdot P)^3 - E \cdot P, \quad (15)$$

where E is the electric field and $r = A(T - T_c)$. The parameters A , B , and C are taken to be positive definite. The system undergoes a second-order ferroelectric phase transition. However, in displacive ferroelectrics such as BaTiO_3 , the polarization vector is strongly coupled to the lattice, so the spontaneous polarization causes a strain which transforms the crystal from a cubic to a tetragonal phase. The elastic modes decay faster than the order parameter and thus can be integrated out, leading to an effective Hamiltonian of the form Eq. (15), with B positive or negative. A negative value of B leads to a temperature-induced first-order ferroelectric transition. An interesting feature of such ferroelectrics is that, in addition to standard hysteresis loops, they exhibit pinched hysteresis loops as the electric field is cycled periodically. This is in accordance with our results (Sec. IV A 2).

The hysteresis loops of good single crystals of ferroelectric BaTiO_3 exhibit rather sharp corners and are distinctly rectangular. The value of the coercive field, measured at room temperature, varies from a minimum of 500 V/cm to a maximum of 2000 V/cm.^{9,10} These experimental values are very much smaller than the value expected on the basis of a simple Landau theory (indicating the relevance of fluctuations of the order parameter). Merz¹¹ found experimentally that the rate at which polarization reversals occur is proportional (at low fields) to the applied electric field. Thus the shape of the hysteresis loop depends on the rate at which the field is cycled. The coercive field is found to increase as a function of the frequency of the cycled field. These qualitative effects are reproduced by our large- N analysis (see the discussion in Sec. IV A 1).

Figure 5 shows the observed hysteresis curves for a crystal of BaTiO_3 where the Curie temperature is 107 °C. When $T > T_c$ and $E=0$, the crystal is in a nonpolar state. The P - E curves are thus linear [Fig. 5(a)] for small fields. When E crosses a critical field strength, a distinct change in polarization occurs and one observes a double hysteresis loop [cf. our [Fig. 3].

Double hysteresis loops and pinched hysteresis loops have been observed in the displacive ferroelectric SbSI.¹² Optical studies and polarization measurements indicate that the ferroelectric transition on SbSI at approximately 20 °C is of first order. The electric displacement versus electric-field hysteresis loops at various temperatures are shown in Fig. 6. It is seen that above the transition temperature, distinct pinched and double hysteresis loops are observed. Note the qualitative similarity between our results (as discussed in Sec. IV A 2) and those obtained from the experiments quoted above.

Our next prediction concerns the scaling of the area of the hysteresis loop with the amplitude of the magnetic (electric) field for low values of the amplitude and frequency. There has been no systematic study of the dependence of the area of the loop with the parameters of the applied field for ferroelectrics, in contrast to the immense amount of work on ferromagnets (see the Introduction). While it is true that real ferroelectrics are more complicated than what our simple model would suggest, we feel that our qualitative predictions should still be applicable. Most ferroelectrics possess strong dipolar

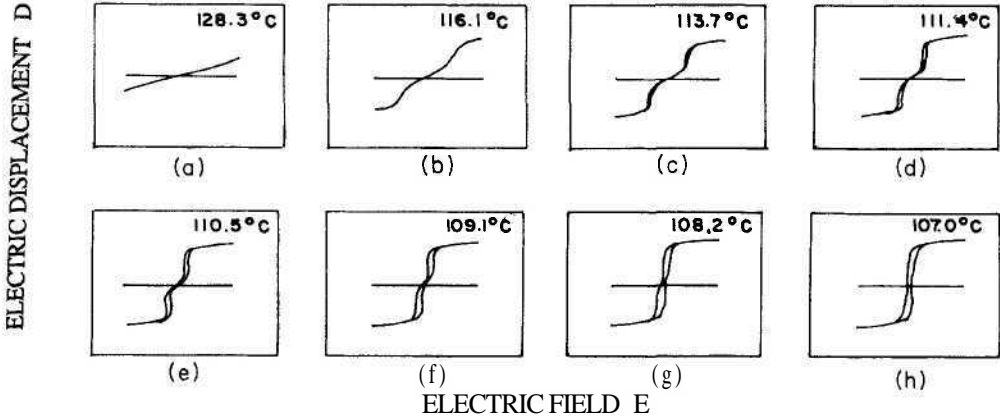


FIG. 5. Hysteresis loops of BaTiO_3 at various temperatures and field strengths (after Merz, Refs. 9 and 11).

forces and lattice²¹ anisotropy effects and are therefore highly anisotropic. We feel that even if these additional complications were included, *a scaling behavior of the area would still exist*, though the numerical value of the scaling exponents would be different (different universality class). It would be very interesting to check for such a scaling behavior for low amplitudes and frequencies in real ferroelectrics.

B. Thermal hysteresis

1. Evolution of shapes as a function of amplitude and frequency

We have carried out a preliminary analysis of thermal hysteresis in the $(\Phi^2)^3$ theory. Equations (12) are solved numerically to obtain asymptotic shapes (hysteresis loops) for various values of parameters. It is convenient to turn on a small magnetic field ($H \approx 10^{-6}$ in dimensionless units) in the $a = 1$ direction of spin space which or-

ders the spins in the $a = 1$ direction in the ferromagnetic phase (in corresponding experiments on CDW systems a small electric field is turned on). We start from the paramagnetic phase and cycle the temperature across the first-order boundary (wings) into the ferromagnetic phase. We compute the magnetization as a function of the temperature r and study its hysteretic response. We note that, keeping the frequency fixed, there is a progression of shapes as a function of the amplitude r_0 . For very small amplitudes (the magnitude of r_0 for which this is true depends on Ω and r , u , and v), the loop is extremely narrow and does not enclose an appreciable area. Within our numerical accuracy, we would claim that the area is zero. As the amplitude increases the loop opens out (see Fig. 7) to give an asymmetric hysteresis loop. This loop is asymmetric about the freezing temperature r_f (unlike the symmetric hysteresis loops of Sec. IV A 1). The area of the loop increases with r_0 . The value of r_0 at which the loop opens out is frequency dependent and decreases as Ω decreases. This is qualitatively similar to the thermal hysteresis loops exhibited by certain CDW systems such as $\alpha\text{-TaS}_3$ (see Ref. 13).

We see from Figs. 7(b) and 7(c) that the loop changes curvature and the magnetization remains constant (analogous to magnetization saturation in magnetic hysteresis) when $M=0$. This is because the magnetization is zero throughout the paramagnetic phase, while it is nonzero and temperature dependent in the ferromagnetic phase. The hysteresis loops are asymmetric because the free-energy is not symmetric under $r_f - r \rightarrow r_f + r$. The thermal hysteresis loops are qualitatively different from the magnetic hysteresis loops. In the single-particle picture, thermal hysteresis corresponds to the motion of the particle from the central well to one of the outermost wells. This gives rise to the observed asymmetry in the hysteresis loops.

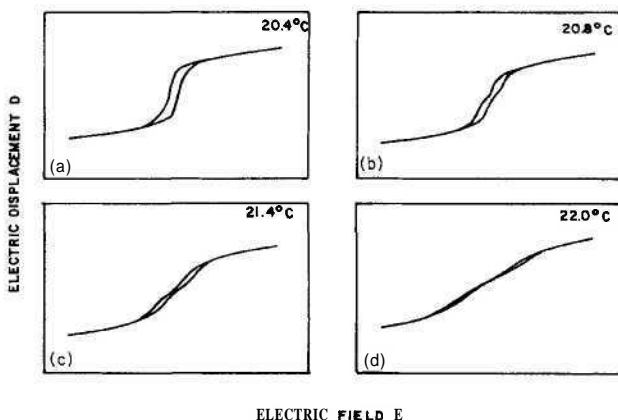


FIG. 6. Hysteresis loops of the ferroelectric SbSI at various temperatures. The ferroelectric transition temperature is at 20°C. Note that as the temperature is increased, the pinched loop evolves into a double loop (after Kawada, Ref. 12).

2. Shape systematics as a function of the parameter u

We can now study the changes in the shape of hysteresis loops as the parameters r and u vary along the

first-order phase boundary. We fix v to be below v_c —this corresponds to the phase diagram shown in Fig. 1. We see that the area of the loop decreases as one moves towards the tricritical point [i.e., as $(r_f, u_F) \rightarrow (r_T, u_T)$]. The reason for this is clear—as we go towards the tricritical point, fluctuations of the order parameter get enhanced. This decreases the coercive field and hence the area of the loop. Furthermore, as we move towards the tricritical point, the jump in the magnetization across the first-order boundary get smaller—this results in a decrease in the remnant magnetization which contributes to a decrease in the area of the loop.

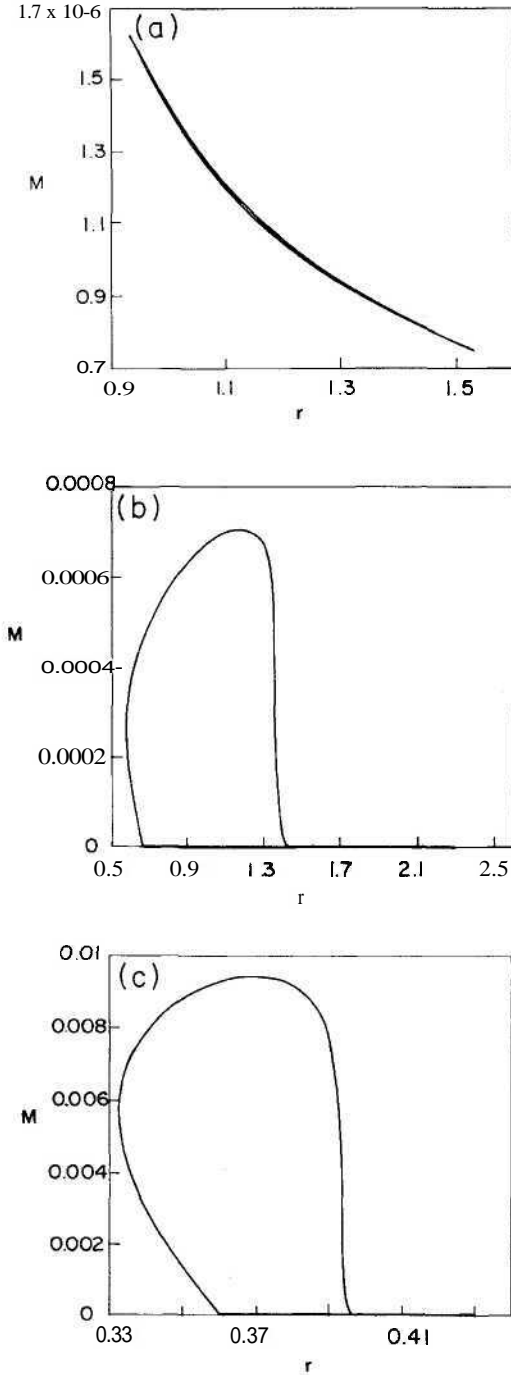


FIG. 7. Thermal hysteresis loops. The loops are asymmetric about the ordering temperature r_f . Note that the loop saturates only on the $M=0$ side of the curve. Ωt is fixed at 5×10^{-3} . (a) $r_f = 1.082$, $\alpha = -23.3$, $r_0 = 0.3$; (b) $r_f = 1.082$, $u = -23.3$, $r_0 = 1$; and (c) $r_f = 0.3824$, $u = -12.766$, $r_0 = 0.1$.

ical point, fluctuations of the order parameter get enhanced. This decreases the coercive field and hence the area of the loop. Furthermore, as we move towards the tricritical point, the jump in the magnetization across the first-order boundary get smaller—this results in a decrease in the remnant magnetization which contributes to a decrease in the area of the loop.

3. Scaling of the area of the hysteresis loop

From the solution of Eqs. (12), we can compute the area of the stable hysteresis loop. This area is a measure of the work done in cycling the temperature through one cycle. Given our earlier work (see Ref. 6 for a discussion), we expect that the area of the hysteresis loop should scale as a function of the amplitude and frequency of the applied field. We see that, as in the $(\Phi^2)^2$ model and the magnetic hysteresis in the $(\Phi^2)^3$ model, the area of the hysteresis loop exhibits a scaling behavior (Fig. 8) as a function of the amplitude of the temperature. We have not done an extensive study to check for the scaling with respect to the frequency of the periodic temperature. Our data are consistent with the scaling law

$$A \sim r_0^\alpha, \quad (16)$$

where $\alpha = 1.0 \pm 0.03$ seems to be independent of the other parameters, namely f_i , u , and v . This scaling behavior is valid for low values of r_0 and Ωt . These exponents should be compared with the scaling exponents one gets for the $(\Phi^2)^2$ model and the magnetic hysteresis in the $(\Phi^2)^3$ model where $f_i = \frac{1}{3}$. We thus conclude that thermal hysteresis of the $(\Phi^2)^3$ model is in a different universality class than the magnetic hysteresis in the $(\Phi^2)^2$ model and $(\Phi^2)^3$ models.

4. Analytical results in the high-frequency limit

We can easily write the integral equations corresponding to the differential equations, Eqs. (12). From these integral equations, one can find the harmonic content of the magnetization, i.e., the different Fourier components of the magnetization. The magnetization and the area can be determined in the large- Ω limit, by an iterative solution of the integral equations. From Eqs. (12), the magnetization in the large- Ω limit is given by

$$M(t) = M_0 \exp \left[-\frac{r_0}{4\Omega} \sin \Omega t \right], \quad (17)$$

where M_0 is the initial magnetization, while the area of the hysteresis loop is given by

$$\begin{aligned} A &= \int_0^{2\pi/\Omega} M(t) \frac{dr}{dt} dt \\ &= \frac{r_0 \Omega M_0}{2} \int_0^{2\pi/\Omega} \exp \left[-\frac{r_0}{4\Omega} \sin \Omega t \right] \sin \Omega t dt. \end{aligned}$$

For large f_i , this can be written as

$$A = -\frac{M_0 r_0}{2} \left[\sum_{n=0}^{\infty} \left[\frac{r_0}{4\Omega} \right]^n \frac{1}{n!} \int_0^{2\pi} \sin^{(n+1)} t dt \right]. \quad (18)$$

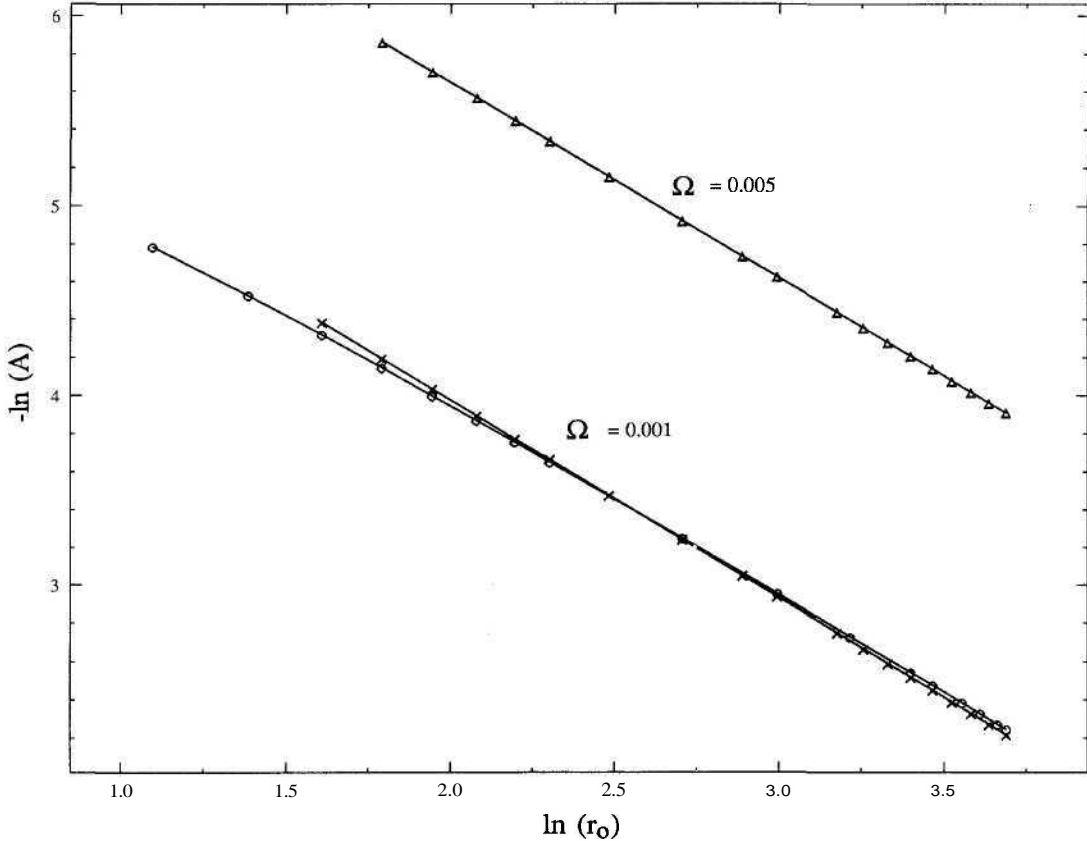


FIG. 8. Scaling of the area of the hysteresis loop as a function of the thermal amplitude r_0 . The slope of the lines gives the exponent a , which is found to be equal to 1, independent of Ω , r , u , and v .

In the $\Omega \rightarrow \infty$ limit, the area A scales as $r_0^{\zeta} \Omega^{-1}$, as in the magnetic hysteresis of the $(\Phi^2)^2$ and $(\Phi^2)^3$ models. This reflects the fact that the high-frequency hysteresis is governed by the decay of the order parameter in a single (quadratic) well, which is the same in the $(\Phi^2)^2$ (magnetic hysteresis) and $(\Phi^2)^3$ (magnetic and thermal hysteresis) theories.

5. Experimental status

Several ferroelectrics display a temperature-induced first-order phase transition (from the paraelectric to the ferroelectric phase). These systems thus display thermal hysteresis when the temperature is altered periodically across the ferroelectric transition temperature. As we mentioned before, the $N=3$ version of our model, Eq. (15), adequately describes the ferroelectric transition in several displacive ferroelectrics. Our study should therefore be of relevance to thermal hysteresis in ferroelectric systems. In particular, the scaling behavior of the area of the thermal hysteresis loop, Eq. (16), could be easily studied.

In recent years^{22–24} there has been a lot of interest in the nonlinear response of conductivity in charge-density-wave systems. A large number of experiments, which in-

clude thermal and electrical history dependence of the Ohmic conductivity σ_0 and thermal and electrical hysteresis of the dielectric function $\epsilon(\omega)$, have demonstrated the existence of metastable states of the CDW. For example, experiments¹³ on the CDW system, orthorhombic TaS_3 , have observed a hysteretic response in the conductivity (in the presence of a small external field) when the temperature was cycled periodically through the Peierls transition temperature. Figure 9 shows the results of the thermal hysteresis experiment. It was observed that the area of the hysteresis loop increased with the amplitude of the periodically varying temperature. Furthermore, the hysteresis loops were asymmetric about the Peierls temperature T_p and did not saturate. The area of the hysteresis loop decreased as the amplitude of the temperature was decreased and was almost zero for very small amplitudes. Extensive experiments have been carried out in other pinned CDW systems such as $NbSe_3$ and $K_{0.3}MoO_3$. It should be mentioned, however, that hysteresis loops in these systems seem to be independent of the rate of temperature variation. This is a reflection of the details of the dissipation mechanism and the nature of pinning.

We see a qualitative similarity between our results for thermal hysteresis in the $(\Phi^2)^3$ theory and those obtained

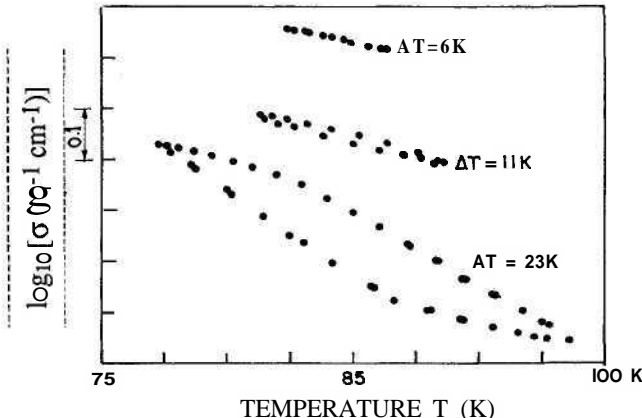


FIG. 9. Typical hysteresis loops of a pure sample of o-TaS_3 for various widths of temperature cycling. Curves are shifted by 0.2 for better visibility (after Hutzler and Mihaly, Ref. 13).

from observing temperature driven hysteresis in CDW systems. However, we have not demonstrated that dynamics of our model Eq. (2) describes nonequilibrium phenomena in CDW systems in any way (as we have done for ferroelectric systems). We can provide heuristic arguments²⁵ to relate our model to a model describing CDW systems when the electric field E , Ω , and temperature T are small. A phenomenological model which explains most experimental data was proposed by Fukuyama²⁶ and Lee and Rice (called the FLR model).²⁷ The model describes an incommensurate, sinusoidal charge-density wave interacting with randomly spaced impurities. If the fluctuations of the randomness are neglected, we recover the rigid model²⁸ of CDW sliding. This model is equivalent to a commensurate CDW in random field. The rigid approximation is useful when the electric field is much smaller than the threshold field ($\epsilon_T \approx 100$ mV/cm in real systems). In the vicinity of the threshold field, fluctuations of the random potential become important. For weak fields, however (much smaller than ϵ_T), the effects of disorder are minimal, and the rigid model is adequate to describe most of the properties. We can demonstrate²⁵ that at zero temperature, our model is equivalent to the dynamics of the FLR model in the rigid approximation. Thus our model describes hysteretic behavior in CDW's in the weak pinning, low-field (much smaller than the threshold field) limit.

The existence of many metastable states, some of them differing in large regions, can naturally give rise to many hysteretic and phase memory effects. It would be useful if one could study the hysteretic properties of the full FLR model (which includes fluctuations of the random potential) both at zero and nonzero temperatures (including thermal fluctuations) so as to make a detailed comparison with the many experiments showing various forms of hysteretic behavior.

Notwithstanding all these cautionary remarks, we would like to claim that our model does have certain qualitative features which are of interest in real CDW systems. We feel that the prediction of a scaling behavior

for the area of the hysteresis loop as function of the amplitude (for low amplitudes) is an important prediction of the model. This can be easily verified by performing experiments on deformable CDW systems such as TaS_3 . The exact value of the exponent (namely $\alpha=1$) may not be seen in experiments, since as we have mentioned, we must be extremely cautious in applying our quantitative results to real CDW systems.

V. COMMENTS

In this paper we have attempted to describe the nonequilibrium statistical mechanics of spin systems driven by an external periodic field across a first-order phase boundary. In particular we have analyzed the hysteretic response of the N -component $(\Phi^2\Phi)^3$ theory. This theory exhibits both magnetic-field-driven and thermally driven first-order phase transitions. Accordingly we study both magnetic and thermal hysteresis. The dynamics of the order parameter is specified by a purely relaxational Langevin equation. Our results are in qualitative agreement with experimental data on magnetic hysteresis in ferroelectrics^{9–12} and on thermal hysteresis in CDW systems.¹³ Our most important prediction is the existence of a scaling behavior of the area of the hysteresis loop at low frequencies and low amplitudes, and high frequencies. We find that the area of the magnetic hysteresis loop scales as H_0^α , where $\alpha=0.6$ for low frequencies and amplitudes. The exponent α is independent of the parameters r , u , v , and $f\Gamma$. This scaling behavior is similar to the scaling behavior exhibited by the $(\Phi^2)^2$ theory. On the other hand, the area of the thermal hysteresis loop scales as $r_0^{1.0}$ for low values of the amplitude r_0 and frequency. Thus thermal hysteresis belongs to a different universality class than magnetic hysteresis. The high-frequency behavior in the two cases is the same—the area scales as $(\text{amplitude})^2\Omega^{-1}$. The precise values of the exponents are model dependent—as yet we have not attempted a detailed classification of the various dynamical models. The *existence* of a scaling behavior of the area is, we believe, shared by these various models and will persist when more realistic models are constructed.

The time scales and the frequencies quoted in the text are measured in units of a microscopic relaxation time Γ^{-1} . The dynamic model is not completely defined until one specifies the nature of the microscopic dissipation. In our study we have taken the kinetic coefficient to be a constant independent of the wave vector (since the dynamics is nonconserved) and frequency, and the parameters of the driving field. In insulating ferromagnetic (ferroelectric) systems, the microscopic dissipation is primarily due to spin (dipole)-lattice relaxations. This relaxation time is of the order of 10^{-8} s in ferromagnets and is smaller in ferroelectrics and can be measured by the width of the ferromagnetic (ferroelectric) resonance line. The reason for the smallness of the relaxation time in ferroelectrics is that the molecules constituting the ferroelectric are strongly coupled to the lattice. Γ should therefore depend sensitively on driving field. This dependence has not been incorporated in our analysis and may not be relevant at low frequencies and amplitudes.

Therefore the theory should be applied with caution when comparing its quantitative predictions with the behavior of displacive ferroelectrics. Ferroelectric systems are highly anisotropic in general—having a strong lattice anisotropy. Moreover, long-range dipolar interactions, responsible for the formation of ferroelectric domains, are the dominant interaction between the molecules of the ferroelectric sample. These additional terms break the rotational invariance of the Hamiltonian and are relevant for the scaling behavior. These interactions, however, should not alter the qualitative predictions of the theory.

In charge-density-wave systems the microscopic dissipative mechanism is generally electron-phonon interactions. This might in general be temperature dependent—this dependence has been neglected in our analysis of thermal hysteresis. Furthermore, Γ for CDW systems might be q and ω dependent^{22,24}—this is, in fact, true for spin glass also owing to the distribution of barrier heights. Let the state of the system be described by a metastable configuration ϕ_0 . A distribution of barrier heights implies a distribution of local threshold fields ϵ_0 (the global threshold field ϵ_T is a maximum of these local fields). When the external field exceeds a certain ϵ_0 , the phases will locally slip until it encounters a barrier whose height is larger than ϵ_0 . For fields ϵ_0 and ϵ_T , these slippages will occur over a larger and larger length and time scales. Thus, for fields between ϵ_0 and ϵ_T , the friction Γ will be q and ω dependent and in fact singular at low frequencies. The value of ϵ_0 depends on the particular

metastable configuration one started out with, since the local environment around these configurations will be different. Real CDW's might thus be expected to exhibit Barkhausen noise²⁹ in their hysteresis behavior—though finite temperature effects might smear out this feature.

ACKNOWLEDGMENTS

M. R. thanks R. Frindt for an interesting discussion on CDW systems and B. Fourcade for critically reading the manuscript. This work was mainly done at the Indian Institute of Science, Bangalore and was funded by the Council for Scientific and Industrial Research, University Grants Commission, and Department of Science and Technology, India. The latter part of the work was completed at Simon Fraser University, Vancouver and was supported by the National Science and Engineering Research Council, Canada.

APPENDIX: PHASE DIAGRAM OF THE $O(N = \infty)$, $(\Phi^2)^3$ MODEL IN THREE DIMENSIONS

In this appendix, we shall outline the calculation of the phase diagram of the three-dimensional, $O(N = \infty)$ symmetric, $(\Phi^2)^3$ model and present numerical details along a cut across the parameter space. Details of the calculation can be found in Refs. 16 and 17. Since our theory is defined on a lattice, all space integrals have a lattice cutoff equal to 1. The partition function of this model can be written as

$$Z_N = \int \prod_{\alpha} d\Phi_{\alpha} \exp \left[- \int d^3x [\frac{1}{2} \nabla \phi_{\alpha} \cdot \nabla \phi_{\alpha} + NP(N^{-1}\Phi_{\alpha}\Phi_{\alpha}) - H_{\alpha}\Phi_{\alpha}] \right], \quad (\text{AD})$$

where

$$\begin{aligned} P(N^{-1}\Phi_{\alpha}\Phi_{\alpha}) &= \frac{r}{2}(N^{-1}\Phi_{\alpha}\Phi_{\alpha}) + \frac{u}{4}(N^{-1}\Phi_{\alpha}\Phi_{\alpha})^2 \\ &\quad + \frac{v}{6}(N^{-1}\Phi_{\alpha}\Phi_{\alpha})^3. \end{aligned}$$

In the limit $N \rightarrow \infty$, the value of the integral is given by its saddle-point value. Since $\Phi_{\alpha} \sim O(N^{1/2})$, the measure increases as an elementary volume in an N -dimensional space. Transforming to $O(1)$ variables R and A , where

$$NR = \Phi_{\alpha}\Phi_{\alpha} \quad (\text{A2})$$

and λ is the Lagrange multiplier enforcing this constraint, we obtain for the partition function (after integrating out of the Φ_{α} variables)

$$Z_N = \int dR d\lambda \exp(-NH_{\text{eff}}[R, \lambda]),$$

where H_{eff} , the effective Hamiltonian, is given by

$$\begin{aligned} H_{\text{eff}}[R, \lambda] &= \int d^3x [P(R) + i\lambda R + \frac{1}{2}\text{Tr} \ln(-\frac{1}{2}\nabla^2 - i\lambda)] \\ &\quad - \frac{1}{4} \int d^3x^3 y H_{\alpha}(x) G(x, y) H_{\alpha}(y). \end{aligned} \quad (\text{A3})$$

$G(x, y)$ is the bare propagator $(-\frac{1}{2}\nabla - i\lambda)^{-1}\delta(x - y)$. We can now perform a saddle-point analysis of the partition function. The saddle-point equations

$$\frac{dH_{\text{eff}}}{dR} \Big|_{R=z, \lambda=i\mu^2} = 0, \quad \frac{dH_{\text{eff}}}{d\lambda} \Big|_{R=z, \lambda=i\mu^2} = 0 \quad (\text{A4})$$

are explicitly given by

$$\mu^2 = \frac{1}{2}(r + uz + vz^2) \quad (\text{A5})$$

and

$$z = \frac{1}{2} \int d^3q [(2\pi)^3 (\frac{1}{2}q^2 + \mu^2)] + \frac{H^2}{4\mu^4} \quad (\text{A6})$$

(the saddle-point solution has been assumed to be homogeneous—this is true when there are no competing interactions). The free-energy density W in the saddle-point approximation is

$$\begin{aligned} W(r, u, v, H) &= \frac{1}{2}rz + \frac{1}{4}uz^2 + \frac{1}{6}vz^3 - \mu^2 z \\ &\quad + \frac{1}{2} \int d^3q (2\pi)^{-3} \ln(\frac{1}{2}q^2 + \mu^2) - \frac{H^2}{4\mu^4}. \end{aligned} \quad (\text{A7})$$

This theory exhibits a low-temperature, ordered phase and a high-temperature, disordered phase. The zeros of the difference of the free energies in the ferromagnetic and the paramagnetic phases determine the phase boundary between the two phases.

1. Ferromagnetic phase

The ferromagnetic phase is characterized by a nonzero spontaneous magnetization. The magnetization is given by

$$M = -\frac{dW}{dH} = \frac{H}{2\mu^2}. \quad (\text{A8})$$

The broken symmetry implies that $\mu^2 = 0$. Therefore

$$z = [-u \pm (u^2 - 4rv)^{1/2}] / 2v \quad (\text{A9})$$

and

$$\mu^2 = [-u \pm (u^2 - 4rv)^{1/2}] / 2v - 1/2\pi^2. \quad (\text{A10})$$

The free energy in the ferromagnetic phase (at $H=0$) is

$$W = \frac{1}{2}rz + \frac{1}{4}uz^2 + \frac{1}{6}vz^3 - \frac{1}{4\pi^2} \left[\frac{2}{9} + \frac{\ln 2}{3} \right]. \quad (\text{A11})$$

2. Paramagnetic phase

This phase has zero spontaneous magnetization. Therefore μ^2 is not equal to zero:

$$z = (1/2\pi^2)[1 - (2\mu)^{1/2}\tan^{-1}(2\mu)^{-1/2}]. \quad (\text{A12})$$

The free energy in the paramagnetic phase (at $H=0$) is

$$\begin{aligned} W_p = & (-\frac{1}{4}uz^2 - \frac{1}{3}vz^3 - \ln 2 / 12\pi^2) \\ & + [3\ln(2\mu^2 + 1) + 12\mu^2 \\ & - 6(2\mu^2)^{3/2}\tan^{-1}(2\mu^2)^{1/2} - 2] / 9. \end{aligned} \quad (\text{A13})$$

We consider those positive roots z of Eq. (A12) for which $\mu^2 > 0$. If more than one root exists, we choose the root for which W_p is the least.

We are interested in the region of parameter space where we expect a first-order phase boundary between the ferromagnetic and paramagnetic phases. In this region u is negative and v is positive. The schematic phase diagram in the $r-u$ plane is as shown in Fig. 1 (for $v < v_c = 16\pi^2$). When $v < v_c$ the critical line intersects the first-order line at the tricritical point, while when $v > v_c$ the critical line terminates at a critical end point. This observation is valid only in three dimensions. We calculate the numerical values of r and u (for fixed $v < v_c$) at the first-order phase boundary (Table I). Our calculations and numerical results are similar to those calculated by Lawrie.¹⁶

¹J. D. Gunton, M. San Miguel, and P. S. Sahni, in *Phase Transitions and Critical Phenomena*, edited by C. Domb and J. L. Lebowitz (Academic, New York, 1983), Vol. 8.

²G. S. Grest, M. P. Anderson, and D. J. Srolovitz (unpublished).

³J. L. Valles, K.-t. Leung, and R. K. P. Zia, *J. Stat. Phys.* 56, 43 (1989).

⁴T. Sun, H. Guo, and M. Grant, *Phys. Rev. A* 40, 6763 (1989).

⁵M. Rao, H. R. Krishnamurthy, and R. Pandit, *J. Phys. Condens. Matter* 1, 9061 (1989); *J. Appl. Phys.* 67, 5451 (1990).

⁶M. Rao, H. R. Krishnamurthy, and R. Pandit, *Phys. Rev. B* 42, 856 (1990).

⁷C. P. Steinmetz, *Proc. Am. Inst. Electr. Eng.* 9, 3 (1982).

⁸R. M. Bozorth, in *Ferromagnetism* (Van Nostrand, New York, 1951).

⁹W. J. Merz, *Phys. Rev.* 91, 513 (1953).

¹⁰H. H. Wieder, *J. Appl. Phys.* 26, 1479 (1955).

¹¹W. J. Merz, *Phys. Rev.* 95, 690 (1954).

¹²S. Kawada, *J. Phys. Soc. Jpn.* 25, 919 (1968).

¹³Gy. Hutziray and G. Mihaly, in *Charge Density Waves in Solids*, Vol. 217 of *Lecture Notes in Physics*, edited by Gy. Hutziray and J. Solyom (Springer-Verlag, Berlin, 1985).

¹⁴V. J. Emery, *Phys. Rev. B* 11, 3397 (1975).

¹⁵S. Sarbach and T. Schneider, *Phys. Rev. B* 16, 347 (1977).

¹⁶I. D. Lawrie, *Nucl. Phys. B* 257, 29 (1985).

¹⁷Madan Rao, Ph.D thesis, Indian Institute of Science 1989.

¹⁸E. A. Novikov, *Zh. Eksp. Teor. Fiz.* 47, 1919 (1965) [Sov.

Phys.—JETP 20, 1290 (1965)].

¹⁹We should think of a temporal noise term providing random kicks to the particle in addition to the external periodic field. The particle will thus be able to jump from one minimum to another even when the amplitude of the external field is smaller than the spinodal field.

²⁰A. F. Devonshire, *Philos. Mag.* 40, 1040 (1949).

²¹While the model we have considered incorporates the coupling of the polarization vector with the lattice, it is implicitly assumed that the elastic modes equibrate faster than the components of the order parameter. This assumption is valid when the frequency Ω and the amplitude H_0 of the applied field is low.

²²D. S. Fisher, *Phys. Rev. B* 31, 1396 (1985).

²³P. B. Littlewood and R. Rammal, *Phys. Rev. B* 38, 2675 (1988).

²⁴P. B. Littlewood and C. M. Varma, *Phys. Rev. B* 36, 480 (1987).

²⁵M. Rao (unpublished).

²⁶H. Fukuyama and P. A. Lee, *Phys. Rev. B* 17, 535 (1977).

²⁷P. A. Lee and T. M. Rice, *Phys. Rev. B* 19, 3970 (1979).

²⁸G. Grüner, A. Zawadowski, and P. M. Chaikin, *Phys. Rev. Lett.* 46, 511 (1981).

²⁹For analogous behavior in ferromagnets see R. M. Bozorth, Ref. 8.